Robot-based Continuous Ultrasonic Welding for Automated Production of Aerospace Structures

Manuel Engelschall, Lars Larsen, Frederic J.C. Fischer, Michael Kupke
Center for Lightweight Production Technology (ZLP), German Aerospace Center (DLR)
Am Technologiezentrum 4
86159 Augsburg

ABSTRACT

Thermoplastic composite materials for structural aircraft components offer advantages in terms of performance and efficient production. In this context, ultrasonic welding is a promising joining technique that could replace the classical mechanical fastening by riveting and bolting which requires extensive drilling and sealing. At the Center for Lightweight Production Technology (ZLP) in Augsburg a robot-based continuous ultrasonic welding system has been developed. It consists of an end-effector mounted on a standard industrial robot, which allows the flexible joining of large flat and double-curved structures. The functional efficiency has already been proven on various components such as a stiffened fuselage panel or a rear pressure bulkhead. In order to benefit from the high welding speed this fusion bonding process is currently being matured to further improve robustness. A parameter study was carried out to identify optimized processing parameters.

1. INTRODUCTION

In today's aircraft production, the large structural components of an aircraft are first assembled and then equipped with the necessary systems. One reason for this sequential assembly is that drilling and riveting of aluminum produces chips and dust, which could damage already integrated electrical and hydraulic systems of the aircraft during operation, e.g. by rubbing up the insulation.

In the future, in order to save costs, the individual sub-components should ideally be pre-equipped with systems when better accessibility is given. Thereby the lead time in final assembly can be reduced since only the finished individual components have to be joined. The use of thermoplastic fiber-reinforced plastics allows components such as skin, stringers and frames to be welded together.

2. STATE OF THE ART

In ultrasonic welding high-frequency vibrations (typically between 20 – 40 kHz) are transmitted via a sonotrode to the sample surface that lead to frictional and viscoelastic heating at the weld interface [1]. The applied pressure as well as the welding time and amplitude are the main process parameters that need to be tune to the respective matrix system.

Energy directors with increased damping are frequently applied to draw the heat energy to the welding area. In this context, Tateishi *et al.* first studied the usage of neat resin interlayer films between weld partners [2]. Villegas *et al.* have tested various energy directors and probed their applicability for ultrasonic welding, especially for CF/PPS [3–6].

The physical phenomena governing the weld process have been intensely probed and modelled to increase process understanding but remain a matter of ongoing research [7], [8].

Other approaches focus on increasing the robustness by additional process control and in-line quality assurance measures [9], [10]. Most studies so far have focused on to static ultrasonic spot welding [11], [12], and only recently continuous ultrasonic welding has been demonstrated on a lab scale [13].

The functionality of the system has been proven in various applications at DLR ZLP. Such as a stiffened fuselage panel or a double curved parts with weld length up to 1500 mm.

With this work, advancement in robot-based continuous ultrasonic welding at the Center for Lightweight Production Technology are presented which aim to render the technology ready for large structural part assembly.

3. EXPERIMENTATION

2.1. End-effector setup

The constituents of the end-effector subsequently acting upon the surface of the weld part are a compaction roller, a sonotrode and a compaction unit, each of which is supported by a pneumatic cylinder that enables up to 3 kN to be introduced into the weld zone. A 20 kHz Branson DCXs 20VRT generator with a maximum power output of 4 kW is used as ultrasonic generator. A sonotrode with a spherical contact area and a diameter of 25 mm was used for these experiments.

Furthermore, the end-effector is equipped with sensors to measure the acting pressures and the setting distances, in order to monitor and control the process during welding. All measured values are recorded at a sampling rate of 1 kHz and the process is controlled at the same speed.

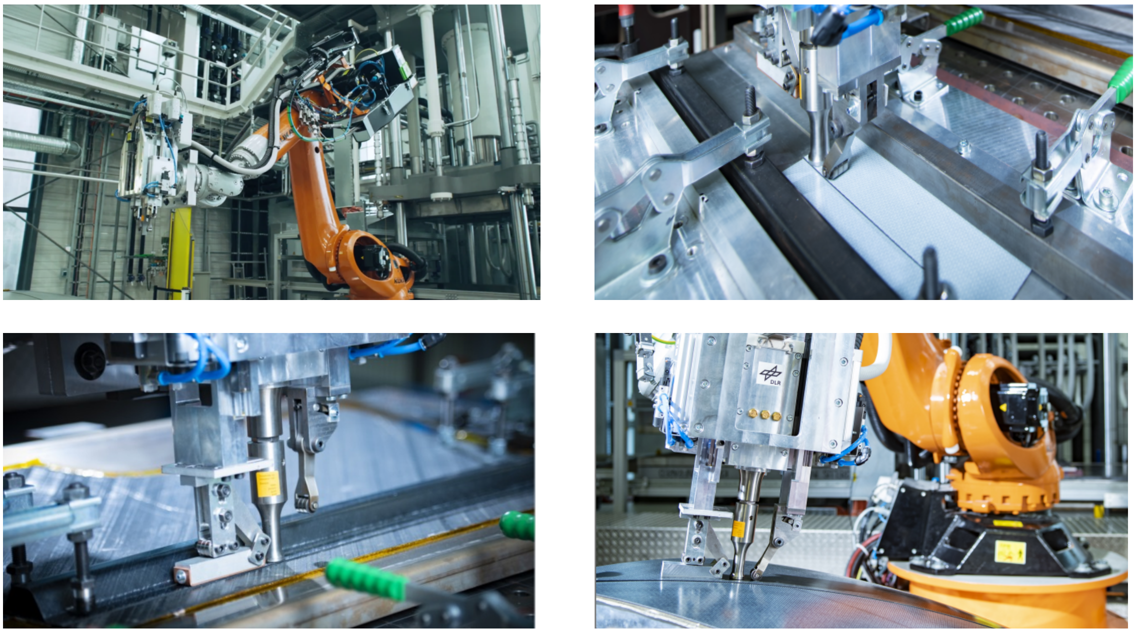

Figure 1: use of the end-effector for various applications: end-effector mounted on robot, flat laminates, stringer on skin, curved parts

2.2 Accuracy measurement

The end-effector was originally mounted to a test bench with a stiff linear axis to minimize travel deviations. For the industrial maturation the end-effector was then set into operation on an industrial robot (type Kuka Quantec KR210 R3100) on a 7 m long linear axis. The accuracy of the robot-based welding process was tested with a Leica Absolute Tracker 901 LR system which measures the pose of the end-effector during the welding process.

To measure the movement of the robot, the end-effector was equipped with a Leica T-MAC30B reflector which was mounted nearby the flange. The tracker can determine the 6-DOF position of the TMAC in its measuring area with a maximal permissible error of 10 µm for distance and 15 µm ± 6 µm for angular performance. The controller of the laser tracker provides the current measurement data with a sample rate of 1 kHz. As measuring software Spatial Analyzer from New River Kinematics was used.

2.3 Parameter study

For the parameter study a test design was setup using DesignExpert8, software for statistical design of experiments. A screening with four factors, namely weld force, amplitude, pressure and travel speed at two levels was performed. The parameters used are listed in Table 1. The force on the compaction roller in front of the horn and the thickness of the energy director (ED) were kept constant.

	Weld Force (F)	Amplitude (A)	Velocity (v)	Consolidation Pressure (pk)	ED thick-ness (ED)	Compaction Device (RF)
low (-)	300 N	95 %	25 mm/s	5 bar	200 µm	300 N
high (+)	600 N	100 %	35 mm/s	8 bar	200 µm	300 N

Table 1: Parameter-Set used for Robot Based Welding

Single lap samples were designed according to ASTM 1002 with an overlap of 12.7 mm (1/2“). Samples were prepared welding two organo sheets with the size of 250 mm x 104 mm to one another. After the water jet cutting, the organo sheets were cleaned with acetone to remove grease and other contaminations and conditioned in a climatic chamber for a minimum of 24 h at 60°C and 0% humidity before the weld process.

As material a standard aerospace grade carbon fiber reinforced TenCate TC1100 polyphenylene sulfide (PPS) laminate was used with a thickness of 1.90 mm and a stacking sequence of $[(0,90)/(\pm45)/(0,90)]_S$. Two layers of neat matrix film with 100 µm thickness were applied as energy director (ED). The joining partners and ED layers were positioned and fixed in a clamping device (Figure 1 upper right) in order to ensure parallel alignment and prevent displacement during the welding process. After the welding process, now the labelled and welded plates are divided into eight individual samples by means of water jet cutting.

4. RESULTS

Lasertracker

Figure 2 shows the results of the accuracy tests of the robotic welding process by means of laser tracking. The y-displacement of the end-effector 90° to the process direction over the welding path is displayed here. The vertical lines with "start" and "end" indicate the beginning and end of the ultrasonic intromission. The horizontal lines indicate the range in which the end-effector moves over the sample. This y-displacement is in a range of 0.12 mm. In the sections before and after the sounding there are larger displacements due to the application of the process forces, after the end-effector is set upon and removed of the weld partners.

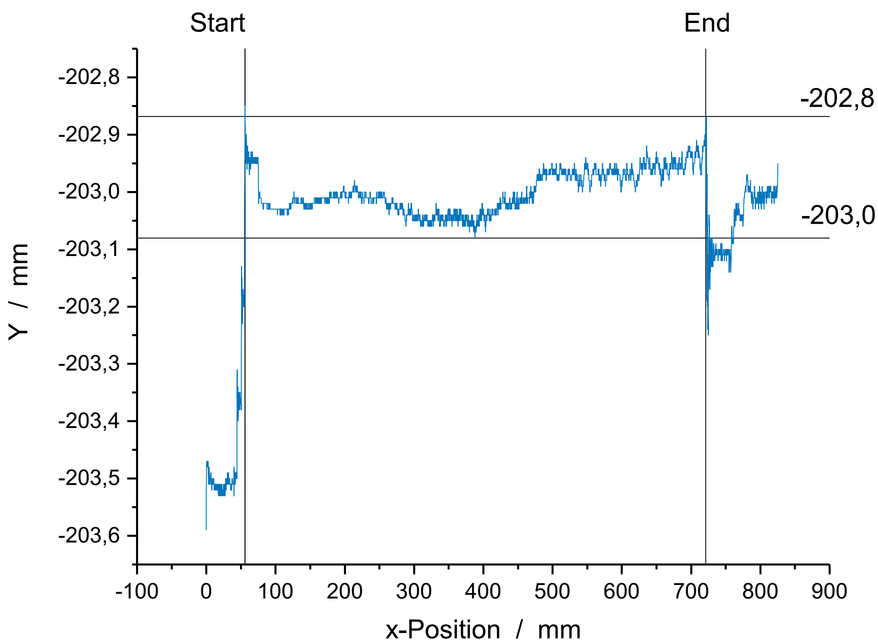

Figure 2: measurement of robot deviation from target value – x-positon robot driving direction, y-position shows deviation perpendicular to driving direction

Parameter Study

The mean of the calculated LSS values for the specimen produced according to the DoE are summarized in Figure 3. The achieved weld strength in MPa is plotted over the numerated test points. The associated welding parameters according to the level of the DoE design are shown above the bar chart. For the calculation of the joining strength the entire surface of the mating weld partners was taken into account, i.e. 12.7 mm by 25.4 mm. The single lap strength was thus not scaled to the actual joined surface in case of partial welding.

The first specimen of each weld run was removed from the analysis since processing conditions are not as uniform after initial intromission at the beginning of the weld process and lead to reduced mechanical properties. This is due to the ultrasonic process itself and the acceleration ramp of the robot.

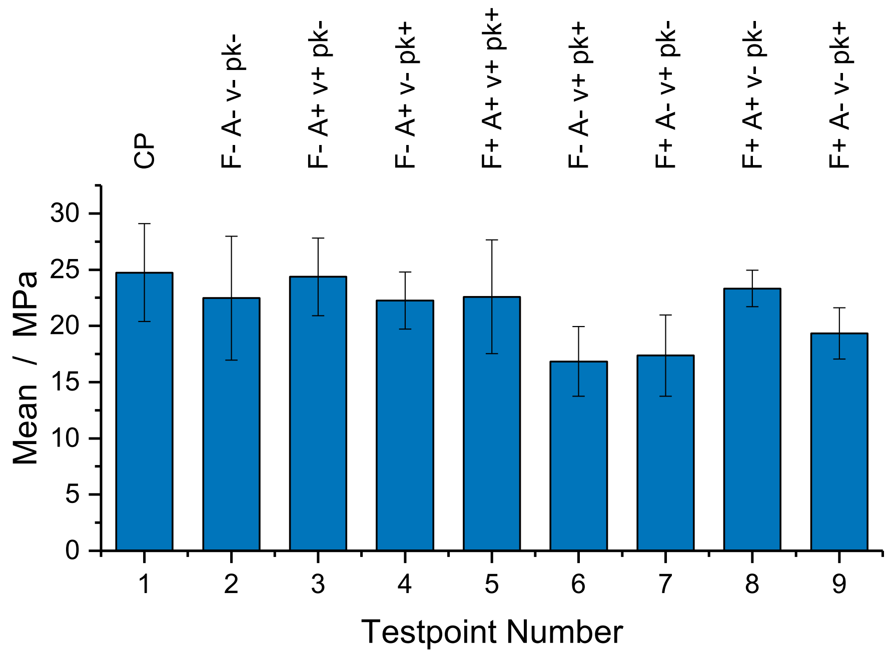

Figure 3 Summary of LSS-Values with corresponding standard devaition and welding parameter

The center point (CP) parameters (F=450 N, A=97.5%, v=30 mm/s, pk=6.5 bar, ED=200 µm, RF=300N) achieved the highest average strength of 24.7 MPa (see Figure 3). With a comparably high joining strength of 23.3 MPa, the parameter set for test point #8 (F=600 N, A=100%, v=25 mm/s, pk=5 bar, ED=200 µm, RF=300N) achieved the lowest scatter over the seven individual specimens with a standard deviation of 1.6 MPa (6.9%).

In general, the samples welded with higher amplitude (100%) show a higher strength. Also the test specimen welded at lower speed, i.e. with 25 mm/s show higher strength values. The runs #5 and #6 show non-welded areas distributed over the joining surface. The samples welded with a weld force of 600 N, amplitude of 95%, a welding speed of 25 mm/s and a compaction pressure of 8 bar (see #9 in Figure 3) only showed partial joining. Here a shifted weld line toward the edge of the upper joining partner, so that merely a band of about 10 mm is welded instead of 12.7 mm.

With the design of experiment software, a potential interaction of the two processing parameters consolidation pressure (y-axis) und weld force (x-axis) was identified. Figure 4 shows the respective contour plot. If both are at the low or high level this leads to higher LSS-values, than parameter set with mixed levels e.g. low consolidation pressure and high weld force, with the highest mechanical properties achieved at low weld force of 300 N and consolidation pressure of 5 bar acting on the compaction unit.

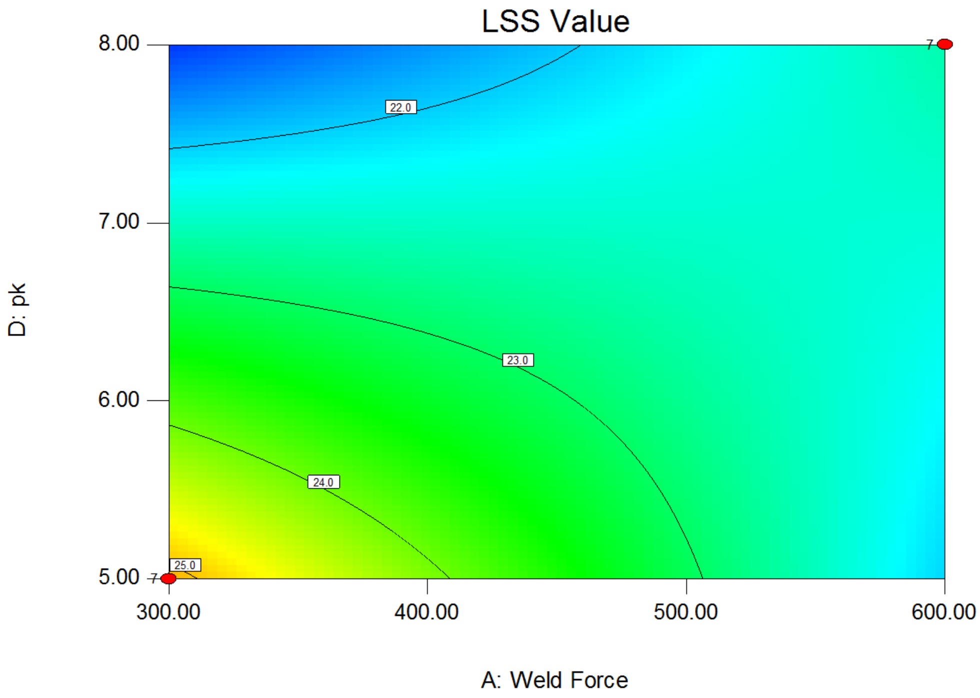

Figure 4: Contour Plot DesignExpert8 correlation between Consolidation Pressure and Weld Force and influence on LSS-Value

5. DISCUSSION

The accuracy measurements carried out showed a satisfactory small y-deviation of 0.12mm over a welding length of 825mm. however, the displacement is greater by the placement of the end-effector and the joining partners, the application of process forces and the start of ultrasonic intromission. For a robust process, the offsets in these areas should be reduced.

The achieved joining strengths of 24.7 MPa at the center Point (F=450 N, A=97.5%, v=30 mm/s, pk=6.5 bar, ED=200 µm, RF=300N) may be compared to 36.5 MPa achieved by static spot welding [14]. In spot welding one often obtains higher mechanical properties as the weld is cooled under pressure which improves consolidation [15]. A welding factor of 0.67 (continuous/spot) is thus achieved in a production relevant environment. Higher mechanical properties are to be expected at slower joining speeds as indicated by the DoE analysis.

For a parameter combination of F=300 N, A=100%, v=25 mm/s and pk=5 bar, ED=200 µm, RF=300N

a strength of 26.7 MPa is calculated by the fitted model. This may be due to higher energy input at prolonged cooling under pressure. These interdependencies of this highly transient process, however, require further investigation and process optimization.

6. CONCLUSIONS

With the developed end-effector continuous ultrasonic welding process was successfully transferred to a robot-based setup. The accuracy of the robotic process was qualified using laser tracker measurements to compare it to the stiff test bench. The displacements in the area of the actual welding process were considered sufficient.

In a first parameter screening performed according to design of experiment highest single lap strength values of 24.7 MPa were determined with the process parameters set to:

F=450 N, A=97.5%, v=30 mm/s, pk=6.5 bar, ED=200 µm, RF=300N

This corresponds to a welding factor of 0.67 as compared to spot welding, and leaves room for further improvement.

The displacement of the end-effector during the welding process shall be tackled in an automated real time correction to minimize the resulting tilting of the end-effector with respect to the contact point via the robot's Remote Sensor Interface (RSI) will be part of the future work.

7. REFERENCES

[1] A. Yousefpour, M. Hojjati, and J.-P. Immarigeon, "Fusion Bonding/Welding of Thermoplastic Composites," *Journal of Thermoplastic Composite Materials*, vol. 17, no. 4, pp. 303–341, Jul. 2004.

[2] N. Tateishi, T. B. Zach, R. T. Woodhams, and T. H. North, "Ultrasonic Bonding of Roll- drawn Polypropylene Using Tie-layers," in *Proceedings of the 47th Annual Technical Conference (ANTEC'89)*, 1989, pp. 496–498.

[3] G. Palardy and I. Fernandez Villegas, "On the effect of flat energy directors thickness on heat generation during ultrasonic welding of thermoplastic composites," *Composite Interfaces*, vol. 2, 2017.

[4] I. Fernandez Villegas, B. V. Grande, H. E. N. Bersee, and R. Benedictus, "A comparative evaluation between flat and traditional energy directors for ultrasonic welding of CF/PPS thermoplastic composites," *Composite Interfaces*, vol. 22, no. 8, pp. 717–729, 2015.

[5] I. Fernandez Villegas and H. E. N. Bersee, "Ultrasonic welding of advanced thermoplastic composites: An investigation on energy-directing surfaces," *Advances in Polymer Technology*, vol. 29, no. 2, pp. 112–121, Jul. 2010.

[6] B. Jongbloed, J. Teuwen, G. Palardy, I. F. Villegas, and R. Benedictus, "Improving Weld Uniformity in Continuous Ultrasonic Welding of Thermoplastic Composites," in *ECCM18 - 18th European Conference on Composite Materials*, 2018.

[7] A. Levy, S. L. Corre, and I. Fernandez Villegas, "Modeling of the heating phenomena in ultrasonic welding of thermoplastic composites with flat energy directors," *Journal of Materials Processing Technology*, pp. 1361–1371, 2014.

[8] G. Palardy, H. Shi, A. Levy, S. L. Corre, and I. F. Villegas, “A study on amplitude transmission in ultrasonic welding of thermoplastic composites,” *Composites Part A: Applied Science and Manufacturing*, vol. 113, pp. 339–349, Oct. 2018.

[9] S. Tutunjian, O. Eroğlu, M. Dannemann, N. Modler, and F. Fischer, “Increasing the Joint Strength of Ultrasonic-spot Welded Fiber-reinforced Laminates by an Innovative Process Control Method,” in *ECCM18 - The 18th European Conference on Composite Materials*, 2018.

[10] F. Fischer, A. Schuster, M. Wilmeroth, R. Glück, M. Engelschall, L. Larsen, and M. Kupke, “Safe and Sound Thermoplastics: Quality Assured Ultrasonic Welding in Fuselage Skin Production,” in *Proceedings of the 18th European Conference on Composite Materials (ECCM 18)*, 2018.

[11] T. Zhao, G. Palardy, I. Villegas, and R. Benedictus, “Towards High-quality Multi-spot-welded Joints in Thermoplastic Composite Structures,” in *ICCM21: 21st International Conference on Composite Materials*, 2017.

[12] T. Zhao, C. Broek, G. Palardy, I. F. Villegas, and R. Benedictus, “Towards robust sequential ultrasonic spot welding of thermoplastic composites: Welding process control strategy for consistent weld quality,” *Composites Part A: Applied Science and Manufacturing*, vol. 109, pp. 355–367, Jun. 2018.

[13] G. Palardy, F. Senders, M. van Beurden, and I. Villegas, “Continuous ultrasonic welding of thermoplastic composite plates,” in *3rd International Symposium on Automated Composites Manufacturing*, 2017.

[14] F. Senders, M. van Beurden, G. Palardy, and I. Fernandez Villegas, “Zero-flow: a novel approach to continuous ultrasonic welding of CF/PPS thermoplastic composite plates,” *Advanced Manufacturing: Polymer & Composites Science*, vol. 2, no. 3–4, pp. 83–92, Oct. 2016.

[15] F. C. Campbell, *Manufacturing Processes for Advanced Composites*. Elsevier Science, 2004.